Disruption mitigation in ASDEX Upgrade with the in-vessel fast valve.

G. Pautasso, D. Coster, X. Bonnin [*], T. Eich, J.C. Fuchs, B. Kurzan, K. McCormick, B. Reiter, V. Rohde and the ASDEX Upgrade Team

Max-Planck-Institut für Plasmaphysik, EURATOM Association, D-85748 Garching, Germany
[*] CNRS-LIMHP, Université Paris 13, F-93430 Villetaneuse, France
e-mail contact of main author: gabriella.pautasso@ipp.mpg.de

Abstract. *The simulation of massive gas injection, done with the 2D transport code SOLPS, allows to calculate the temporal evolution of the total (free plus bound) electron density profile. The calculations show that a volume averaged total electron density, of the order of magnitude of the so-called "Rosenbluth density", can been reached in ASDEX Upgrade after the injection of neon with a fast valve in disruption mitigation experiments. This result supports the possibility of suppressing runaway electrons generated during the current quench in ITER by the simple method of massive gas injection.*

1. Introduction

Plasma disruptions have three major negative effects on a tokamak: large mechanical forces, thermal loads and the generation of runaway electrons. Experiments on ASDEX Upgrade (AUG) and other tokamaks have shown that the magnitude of these effects can be significantly reduced by the massive injection of noble gases (MGI). The injected gas influences the evolution of the plasma disruption since it increases the plasma density and cools the plasma by dilution and radiation before the spontaneous thermal quench occurs. For both types of load - mechanical and thermal - the crucial parameters are the magnitude and the speed of increase of the electron density in the plasma. Among the three disruption effects in ITER, the suppression of the runaway avalanche poses the most severe requirement for the density increase. According to our present knowledge, a disruption in ITER is going to convert a large fraction of the plasma current into a beam of highly energetic runaway electrons. In order to prevent the generation of the runaway electrons, the total (free and bound) electron density, $n_{e,tot}$, must be increased up to the so-called "Rosenbluth density" $n_R \sim 4.2 \times 10^{22}$ m^{-3} [1], which is a factor of 400 larger than the nominal one. It has not been proven yet that this high density can be reached over the whole plasma in present tokamaks and in ITER. In addition such a density is going to significantly affect the design of the pumping system and the reconditioning of the machine after such a shutdown will be time consuming during operation. Therefore it is important to understand which processes control the assimilation of the injected gas by the plasma and its transport into the plasma core in order to maximize them.
Electromagnetic (EM) actuated gas valves have been mostly used in tokamaks for disruption mitigation with impurity gas. They are robust and fast but they must be located in a region of low magnetic field and therefore meters away from the plasma. In ITER the long time delay of the gas travelling along a tube several meters long and the low initial delivery rate may prevent their use. For these reasons a new piezo-released valve, having the advantages of an electromagnetic valve (fast opening and high delivery rate) and being able to operate in the vessel close to the plasma, was developed and installed on AUG in the spring of 2007. The EM valves, located outside of the vessel, and used previously on AUG, are described in [2].
The new valve, which allows to reach electron densities of interest for the collisional suppression of the runaway electrons in ITER and can initiate the current quench within 2 ms from the trigger, is presented in Section 2. Experimental effort has concentrated on documenting the dependence of the fuelling efficiency on plasma and gas parameters: Section 3 describes these results. Modelling has started and allows us to calculate the density evolution of electron, ion and neutral density profiles which all contribute to $n_{e,tot}$. In Section 4 we present the results of the simulation and argue that a volume averaged $n_{e,tot} \sim O(n_R)$ can be reached in AUG with the present in-vessel fast valve.

2. The in-vessel valve

A new piezo-released valve, able to operate close to the plasma, was designed and built by the German company IGAM in collaboration with IPP.

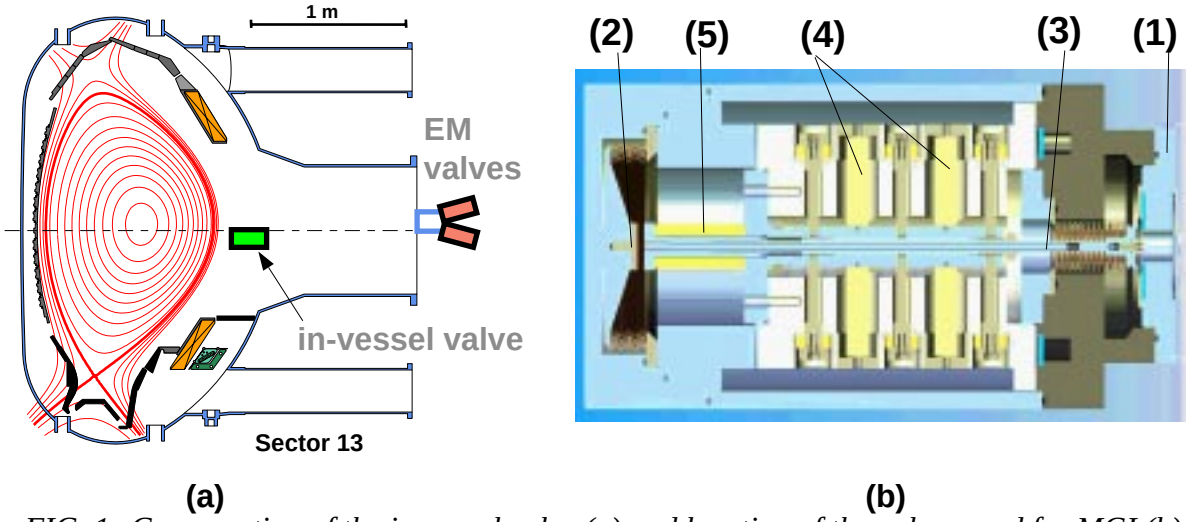

FIG. 1: Cross section of the in-vessel valve (a) and location of the valves used for MGI (b).

The in-vessel valve is a completely new development and satisfies very demanding functional requirements, such as a short opening time (of the order of 1 ms), a large orifice (14 mm of diameter) and practically no leakage ($< 10^{-9}$ mbarl/s). In addition the valve must maintain its full functionality and work under severe environmental conditions, such as high temperature (up to 150 ^{o}C during the baking of the vessel), strong magnetic field and high vacuum (p$< 10^{-7}$ mbar). The valve is located on the low field side of the torus, at the midplane, 5 cm behind the limiting surface defined by the ICRH antenna and 10 cm from the plasma (Fig. 1 (a)). It can operate with a gas pressure of 50 bar and inject up to 4 barl of gas within a few ms. It is the first valve of this type ever used close to the plasma on a tokamak.

The valve, whose sectional view is shown in Fig. 1 (b), consists of
1) a gas chamber, with a volume of 80 cm^3, reduced to 40 cm^3 in some experiments;
2) a pneumatic piston, driven by pressurized air, used to exert pressure on
3) a movable stem, which closes the orifice of the valve;
4) four independent pairs of piezo-actuators, which expand under an applied voltage and hold the stem in the closed-valve position;
5) a disk spring package, which opens the valve - as soon as the piezo-actuators are discharged - by moving the stem away from the orifice.

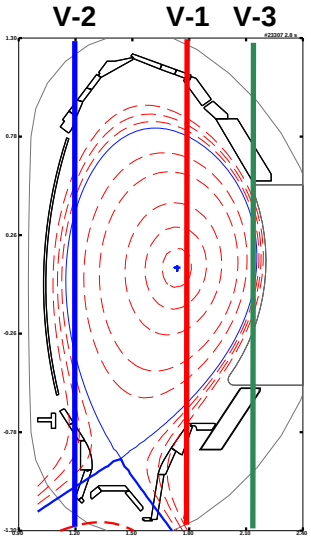

FIG. 2: Vertical chords of the CO_2 diagnostic.

The valve is water cooled, since it is going to be exposed to up to one MW/m^2 of power flux during 8-10 s. It is equipped with a remote controlled gas mixing system, which allows to mix two types of gas in a reservoir and fill the valve just before the discharge. A control unit monitors the charging currents of the piezo-actuators by comparing the actual values with reference ones, which are stored in a flash memory of the micro controller during a calibration procedure. In case of breakdown of one of the actuator pairs, the control unit excludes it from operation. Two of the four pairs of piezo-actuators are redundant to allow the operation of the valve in case of their partial failure. This security margin

is dictated by the fact that the valve is mounted inside the vessel and cannot be accessed for maintenance during the whole experimental campaign (up to 10 months).

3. Dependence of the fuelling efficiency on plasma parameters

The CO_2 laser interferometer is the only diagnostic on AUG able to follow the fast increase of the electron density after MGI. It measures the line integrated density along three verti-

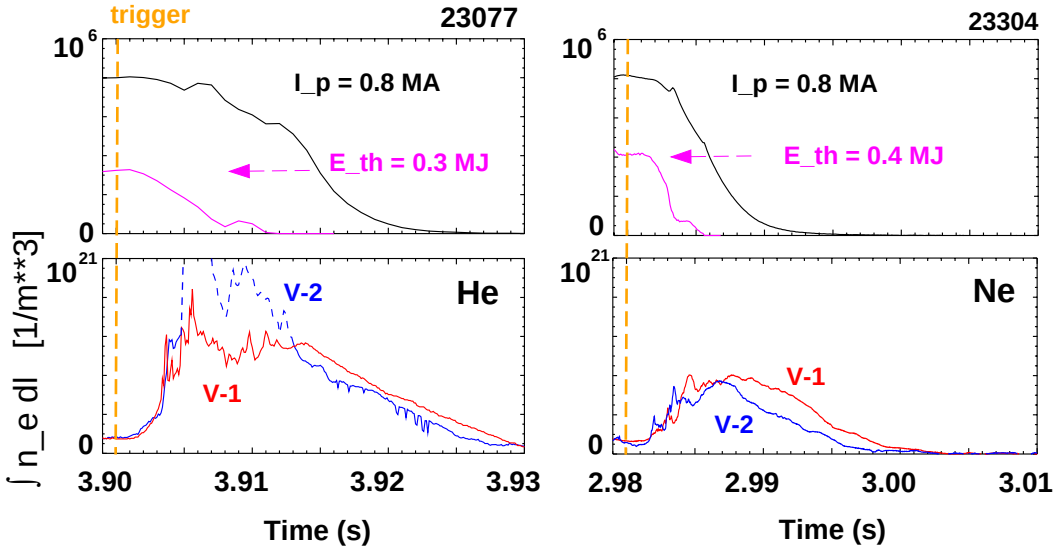

FIG. 3: Time traces of plasma current (I_p), thermal energy (E_{th}) and line integrated density (chords V-1 and V-2 of the CO_2 interferometer) after injection of 0.4 barl of He (left) and Ne (right).

cal chords (see Fig. 2) with a time resolution of 10 μs. The evolution of the density profile cannot be reconstructed from these measurements alone but can be inferred by means of simulations (see Section 4). The measurement from the most central channel (called V-1), i.e $\int n_e\, dl_{V-1}$, is used in the following to define the fuelling efficiency (F_{eff}) as the increase in the total number of electrons divided by the total number of injected gas atoms (or molecules, in the D_2 case):

$$F_{eff} = \frac{\Delta N_e}{N_{inj}} = \frac{\Delta \int n_e\, dl_{V-1}}{N_{inj}} \frac{Vol}{l_{V-1}} \qquad (1)$$

where Vol is the plasma volume and l_{V-1} is the length of the most central chord V-1. F_{eff} could be larger than one, if the injected gas were multiply ionized; in reality the F_{eff} inferred in MGI experiments is significantly smaller than one.

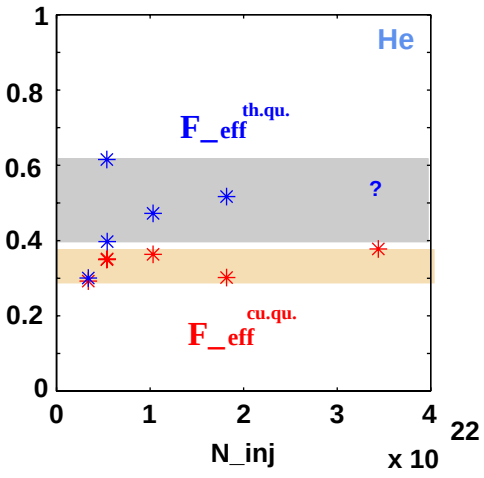

FIG. 4: Fuelling efficiency, averaged over the thermal quench (th.qu.) or over the whole current quench (cu.qu.) as function of the injected number of He atoms

The experiments presented in this paper were mainly made to study the dependence of F_{eff} on the following plasma and gas parameters: distance between plasma and valve, gas pressure in the valve, type of gas, gas quantity and plasma energy.

A series of similar discharges in H mode was shut down by massive gas injection. The valve was triggered towards the end of the current flattop, in plasmas with a toroidal current of 0.8 or 1.0 MA and $q_{95} = 5.7$ or 4.3. The plasma, heated by 5

or 20 MW of NBI power, had a target density of 0.6 or $1 \times 10^{20}\ m^{-3}$, a thermal energy in the range 0.2-0.8 MJ and a magnetic energy of 1 or 1.6 MJ.
Pure deuterium (D_2), helium (He), neon (Ne), and mixtures of Ne and Ar with D_2 have been injected varying the gas pressure in the valve.

Dependence of F_{eff} on distance plasma - valve. The comparison between the old and the new valve was carried out between similar shots with the injection of 0.4 barl of gas (that is 10^{22} atoms) within 5 ms. The striking differences between the shutdown induced by the new and the old valves are that with the in-vessel valve

• the delay time between trigger and start of the current quench is practically eliminated; the current decay induced by the new valve starts 1 ms after the trigger, that is as soon as the valve is open;

• the rate of induced current decay is twice the one observed with the old valves. It is known that the faster the current decay of an elongated plasma is, the smaller is the vertical force on the vessel;

• F_{eff} is 3-4 times higher and the rise of the plasma density starts as soon as the valve opens;

• the maximum radiated power reaches 0.5 GW and is a factor of two higher than with the old valve.

Dependence of F_{eff} on gas pressure. The gas volume in the valve was increased from 40 to 80 ml between the 2007 and 2008 experimental campaigns to allow for the injection of a larger quantity of gas. The same amount of Ne was injected with a gas pressure of 5 and 10 bar in similar target discharges. In the lower pressure case the density rise was slower and the delay between trigger and start of the current quench was longer (3 instead of 2 ms), but the resulting maximum electron density was similar in the two cases.

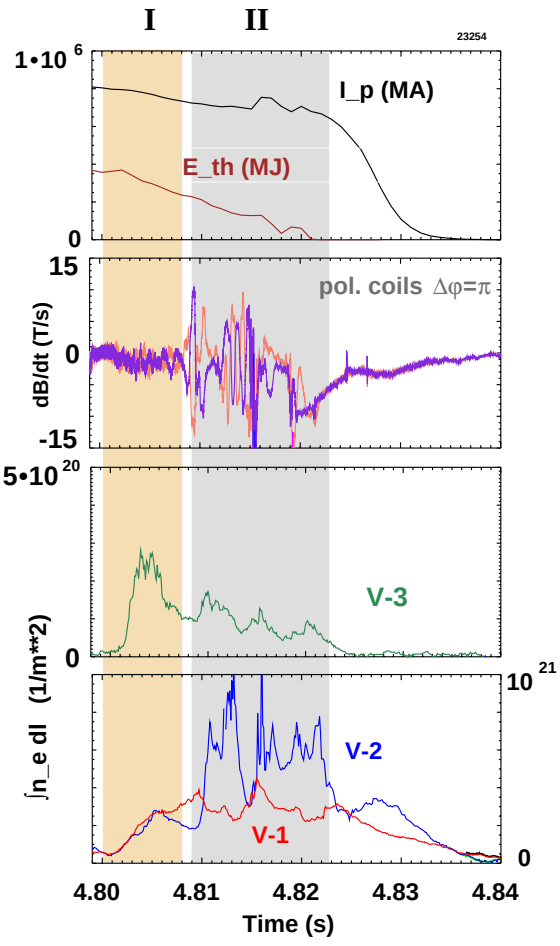

FIG. 5: Time history of plasma current (I_p), thermal energy (E_{th}), Mirnov coil signals and line integrated density after the injection of 0.2 barl of He

Dependence of F_{eff} on N_{inj}. Different quantities of He and Ne, ranging from a total amount of 3×10^{21} up to 4×10^{22} atoms have been injected varying the pressure in the valve from 1.7 up to 40 bar. A line integrated electron density of 2×10^{21} m^{-2} and 10^{21} m^{-2} (l_{V-1} = 1.4 m) has been reached with the injection of 1.4 barl of He and 1.6 barl of Ne respectively. The F_{eff} averaged about the thermal quench (from the start of the thermal quench up to the decay of 20 % of I_p), $F_{eff}^{th.qu.}$, has a large scatter, because of large oscillations in the density measurements, not reproducible from shot to shot, but does not depend on N_{inj} in the scanned range of parameters. $F_{eff}^{th.qu.}$ ranges between 40 and 60 % for He and between 20 and 40 % for Ne. $F_{eff}^{cu.qu.}$, that is averaged over the whole current quench, is a factor of 2 smaller than $F_{eff}^{th.qu.}$ (Fig. 4).

Dependence of F_{eff} on thermal energy . F_{eff} does not show any clear dependence on the thermal energy of the target plasma in the range 0.2-0.8 MJ scanned.

Dependence of F_{eff} on the type of gas. The F_{eff}s of He and Ne have been investigated more extensively than the ones of other gases and mixtures. As already pointed out, He is twice more efficient than Ne and also D_2 in increasing n_e (see

atoms/s	D_2 close	D_2 far	He close	He far	Ne close	Ne far
10^{23}	47%	-	153%	-	210%	-
10^{24}	37% Δt=1 ms	34%	91%	84%	92%	51%
10^{25}	25% Δt=1 ms	-	35%	-	29%	18%

TABLE. 1: *Dependence of F_{eff} on the flow rate, type of gas and valve position.*

Fig. 3).
A series of experiments was carried out to investigate the mitigation and fuelling efficiency of mixtures of D_2 (20%, 50% and 80%) and Ne or Ar. Mixtures of a low-Z and a high-Z gas are found to be as efficient as high-Z injection in quenching the current in other tokamaks (see for example Ref. [3]), since they increase the density of the plasma more than the high-Z alone.
This is not the case in AUG. The time delay between the trigger and the start of the current quench increases with increasing percentage of D_2 in the mixture. The rate of thermal energy dissipation, the rate of the current quench and the radiated power increase with increasing concentration of Ne or Ar. Nevertheless, the F_{eff} is not a monotonic funcion of the concentration of the high Z impurity since the mixture of 50 % of Ne or Ar show a larger F_{eff} than the pure gases alone.
Dependence of F_{eff} on MHD modes. After the injection of a large amount of high Z gas, the thermal quench occurs while the electron density is rising. Whether the large amplitude magnetic fluctuations during this phase influence the assimilation and transport of the gas is an open question. A shut down after a moderate amount of He injection, in which the density rise phase and the thermal quench are not simultaneous, is shown in Fig 5. In this case, the density rise (phase I) is completed when large MHD activity (phase II) starts. The edge chord V-3 shows a strongly modulated but gradual decay of the density, apparently not affected by the MHD activity. The chord V-2 views a region of high density, also seen by the fast camera as a radiating structure poloidally localized on the inner wall (MARFE). This strong poloidal asymmetry persists during the whole MHD activity. There is no evidence from the CO_2 measurements that magnetic fluctuations favour the redistribution of the density towards a flat profile during phase II.

4. Simulations

The code package SOLPS [4] is used to model MGI in AUG and to compare the code results with the experimental measurements. The gas valve is treated as a point source and the neutral gas behaviour is modelled by the Monte Carlo module of the code, Eirene. The valve location, the quantity and the type of gas are treated as parameters and varied to assess their influence on the plasma density response. The code solves the transport fluid equations for the main plasma and impurity species along with a full description of the atomic and molecular processes in a 2D geometry. Gas ionization, density diffusion and plasma cooling are calculated accordingly. Large MHD activity and turbulence strongly modify the transport properties during impurity injection. We treat the heat and particle transport coefficients as parameters and vary them to test their influence on the fuelling efficiency. Experimental measurements of the density and thermal energy evolution are compared with the code predictions.
A parametric study. The first series of simulations is a parametric study aimed at understanding the dependence of F_{eff} on the properties of the injected gas. These simulations consist of injecting a constant flow of gas particles in the target plasma and in modelling the plasma evolution for Δt =3 ms (if not otherwise specified in Table 1). The gas parameters scanned are:

1) the gas flow, dN_{inj}/dt, set equal to 10^{23}, 10^{24} or 10^{25} atoms/s;
2) the type of gas, chosen as D_2, He or Ne;
3) the distance of the valve from the plasma and the divergence of the gas flow. The valve is modelled as a point source of mono-energetic atoms. A Maxwellian distribution of their velocity, which can play a role for valves far from the plasma, has not been implemented yet. In the case labeled "close" in Table 1 the valve is located at R = 2.25 m and the gas flow has an expansion angle $\alpha = \pi/4$; in the case "far" the valve is located at R = 2.50 m and $\alpha = \pi/2$. The plasma separatrix intersects the midplane at R = 2.15 m on the low field side.
The target plasma is obtained by feedback controlling the separatrix density at the outer midplane at about 1.5×10^{19} m^{-3} and heating a standard lower X-point AUG plasma with 5 MW. The resulting plasma has a thermal energy of 290 kJ and H-mode-type n_e and T_e profiles, as in the actual experiments. In this work we limit the simulation to the first 3 ms of the process of gas injection and we neglect the input ohmic power associated with the decay of the plasma current, which becomes significant at a later time.
The F_{eff} calculated after 3 ms of constant gas injection is summarized in Table 1. It is found that:
• F_{eff} decreases significantly with the increase of the rate of injected gas, dN_{inj}/dt. The higher gas flow causes a larger cooling effect, a faster drop of the temperature and the recombination of multiply ionized ions. In the case of injection of 10^{25} atoms/s of He and Ne the thermal energy of the plasma has dropped by 92 and 86 % respectively; the corresponding average ionization charge of the impurities has dropped to 1.1 for both gases after 3 ms of gas injection. The F_{eff} also decreases during the simulation for all three gas species, more significantly at larger gas flows. In the AUG experiments this dependence is not found. The ohmic heating, ignored in this simulation, increases with gas rate and might account for the discrepancy.
• The dependence of F_{eff} on dN_{inj}/dt is stronger at higher impurity atomic number. A comparison of the time evolution of the density and electron temperature profiles after 1 ms of gas injection (see Fig. 6) shows that He and Ne penetrate deeper than D_2 and cool the plasma more, Ne more than He. Experiments on AUG indicate that F_{eff} is larger for He than for Ne, as predicted by these simulations.

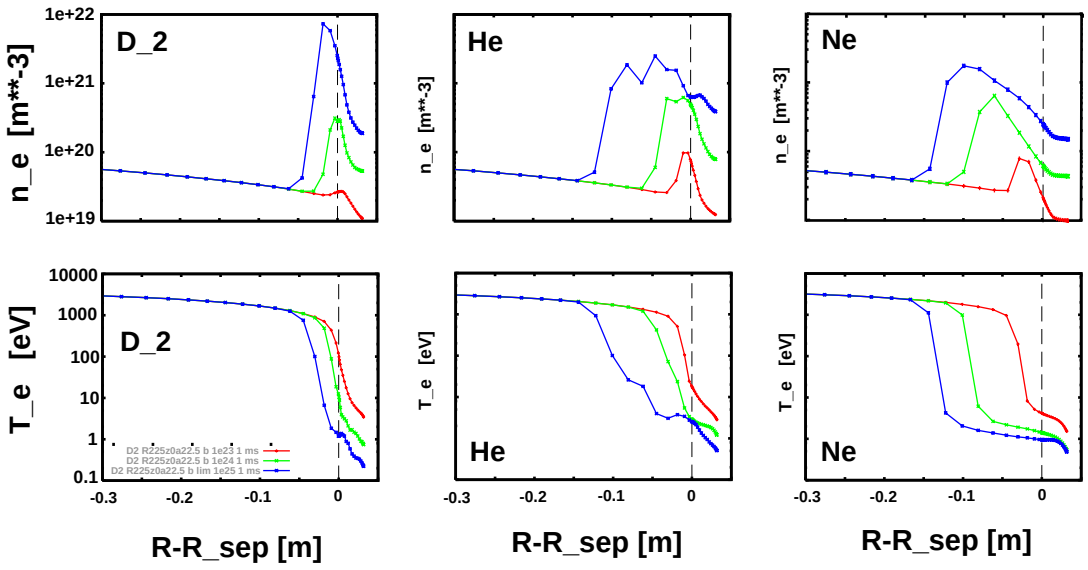

FIG. 6: Profiles of electron density (n_e) and temperature (T_e) at 1 ms for D_2, He and Ne and $dN_{inj}/dt = 10^{23}$ (red), 10^{24} (green) and 10^{25} (blue curve) atoms/s.

• F_{eff} is always less than 50 % for D_2, because of the back-scattering of one of the neutrals during the process of dissociation of the molecule.

• The F_{eff} is larger than 100% only at the low gas flows of $dN_{inj}/dt = 10^{23}$ atoms/s for He and Ne . In these cases the impurity atoms have a degree of ionization Z = 1.9 and 2.5 respectively at t_{SOLPS} = 3 ms.
• F_{eff} decreases significantly for Ne - less for D_2 and He - if the valve is moved away from the plasma and if the flow divergence increases. This is mainly a geometric effect. The transit time of the gas becomes a significant fraction of the simulation time when the valve is placed further away from plasma: Ne reaches the plasma after 0.8 ms when the valve is located at R = 2.5 m. In addition when the flow divergence is large (e.g. $\alpha = \pi/2$), the gas atoms, exiting the valve, reach the plasma spread over a time interval $\Delta t_\alpha = d(1 - cos\alpha)/c$. With a distance between valve and plasma d = 1.5 m, $\alpha = \pi/2$ and a sound speed $c = 400$ m/s then Δt_α = 0.7 ms.
In AUG the valves located outside of the vessel (d = 1.5 m) exhibit a F_{eff} much smaller (factor of 2-3) than the in-vessel valve located close to the plasma. The simulation suggests that a fraction of the atoms injected by the valve outside of the vessel does not even reach the plasma because their trajectories do not intersect it. Another fraction reaches the plasma after the first atoms - the faster and perpendicularly directed - have caused the thermal quench and does not ionize.

Modelling a realistic shut down. A second series of simulations aimed at modelling a specific discharge (shot 21758) in which a plasma (plasma current of 0.8 MA and thermal energy of 290 kJ) was shut down with 0.4 barl of Ne within a few ms. In this simulation the valve is located close to the plasma and it is assumed to open instantaneously. The gas flow is approximated by: $dN_{inj}/dt = 6.9 \times 10^{24}$ atoms/s for t_{SOLPS} = 0-1 ms and $dN_{inj}/dt = 1.2 \times 10^{24}$ atoms/s for t_{SOLPS} = 1-3 ms.
The diffusion coefficients are also changed in this series. The experimental measurements of density and temperature are not detailed enough to allow any inference of the diffusion coefficient profiles. Nevertheless, the SXR emission, measured along chords, shows that a cold front propagates from the plasma edge to the plasma center starting at 0.7 ms and that the central temperature finally collapses at t_{SOLPS} =1.5 ms. The MHD activity also strongly rises around t_{SOLPS}=1.5 ms.
For studying the influence of the loss of confinement on the F_{eff}, the electron heat diffusion coefficient χ_e was changed from the profile of the steady state discharge to values of 100 - 10000 m^2/s constant over the plasma surface at t_{SOLPS} = 1.5 ms from start of injection. $\chi_e = 1000$ m^2/s causes a thermal quench of a duration similar to the one experimentally observed. The effect of the energy quench would be to stop the ionization of the neutrals and to decrease F_{eff}, if it started before most of the particles have reached the plasma. In our case the thermal quench begins after most of the injected gas has reached the plasma and does not have a significant influence on the maximum F_{eff} achieved during the 3 ms.

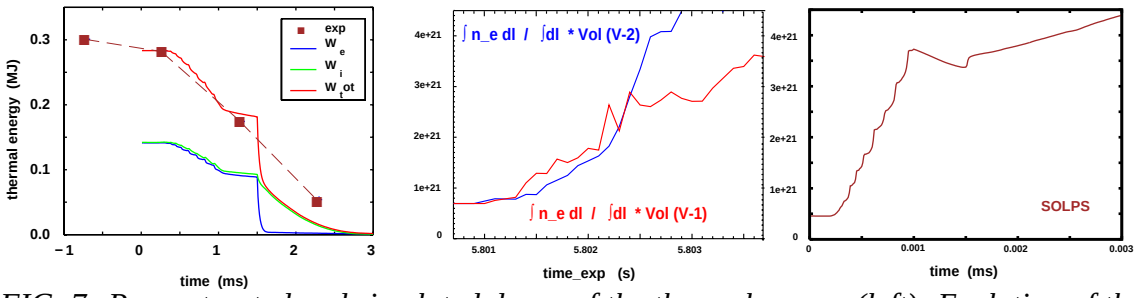

FIG. 7: Reconstructed and simulated decay of the thermal energy (left). Evolution of the total number of electrons, N_e, extrapolated from the V-1 and V-2 chord measurements (center) and simulated $N_e = \int n_e \, dVol$ (right)

The F_{eff} at 3 ms is 42 % and is in agreement with the increase of the total number of electrons inferred from the CO_2 data. The exact time behavior of the line integrated density could not be exactly reproduced even by varying the profile and the magnitude of the particle diffusion coefficient (D_e = 0.1 - 100 m^2/s). This issue will be the subject of further work.

atoms/s	$N_{\mathrm{Ne,i}}$	$N_{\mathrm{Ne,o}}$	$N_{\mathrm{Ne,i}} + N_{\mathrm{Ne,o}}$	$\Delta n_{\mathrm{e,tot}}$ m^{-3}	Y
10^{23}	2.5×10^{20}	4.0×10^{19}	2.9×10^{20}	1.7×10^{20}	97%
10^{24}	1.6×10^{21}	6.8×10^{20}	2.3×10^{21}	1.3×10^{21}	77%
10^{25}	8.6×10^{21}	8.8×10^{21}	1.7×10^{22}	1.0×10^{22}	57%

TABLE. 2: *Assimilation efficiency of the Ne, $Y = (N_{Ne,i} + N_{Ne,o})/N_{inj}$, for different gas flow rates. $N_{Ne,i}$ is the total number of neon ions ionized, $N_{Ne,o}$ is the number of neutral neon atoms and $\Delta n_{e,tot}$ is the increase of the averaged total electron density.*

Total electron density. The free electron density can be measured and the comparison with the simulated value can be used to validate the code calculation. Nevertheless, the bound electrons as well as the free, contribute to the *stopping power* of the plasma for runaways. The number of bound electrons, of which we do not have measurements, can be computed with SOLPS as sum of the contributions from the partially ionized atoms and from the neutrals. Table 2 summarizes the assimilation efficiency of the Ne gas from the plasma ("close" valve), defined as $Y = (N_{Ne,i} + N_{Ne,o})/N_{inj}$, for different gas flow rates. $N_{Ne,i}$ is the total number of neon ions ionized in the plasma and $N_{Ne,o}$ is the number of neutral neon atoms. Y decreases with the increase of the injected number of atoms.
The maximum amount of Ne atoms (Z =10) injected in AUG up to now amounts to 1.6 barl, i.e. 4×10^{22} atoms; with a computational (core + SOL) plasma volume of 17 m^3 and assuming $Y =$ 45 %, consistent with the values of Table 2, then the average total electron density increase is $\Delta n_{e,tot} \simeq n_{e,tot} = 10^{22}$ m^{-3}.
The in-vessel valve allows the injection of 4 barl of gas, equivalent to 10^{23} atoms. In the case of Ne injection and Y = 45 %, the expected $\Delta n_{e,tot}$ is larger than n_R.

5. Summary

This first series of simulations of massive gas injection, performed with the 2D fluid code SOLPS, shed light on the relevant mechanisms limiting the fuelling efficiency. The dependence of F_{eff} on the amount of injected gas, on the gas species and valve position are explained. The injected Ne carries many electrons and is potentially a candidate for raising F_{eff} above 100 %. Nevertheless, its strong cooling effect keeps the electron temperature at a few eVs, its average degree of ionization is close to 1 and the resulting F_{eff} is around 20-40 % for $N_{inj} = 0.4$ - 1 barl. However, a factor of Z (Z=10 for Ne) larger number of electrons is available in the background to suppress the runaway avalanche. A large assimilation factor is computed with SOLPS in the range of injection rates of interest and leaves open the possibility of using MGI for the collisional suppression of runaway electrons in ITER.

References

[1] T.C. Hender et al., Nuclear Fusion **47** (2007) 128-202

[2] G. Pautasso et al., Nuclear Fusion **47** (2007) 900-913

[3] R. Granetz et al., Nuclear Fusion **47** (2007) 1086-1091

[4] R. Schneider et al., Contrib. Plasma Phys. **46** (2006) 3, DOI 10.1002/ctpp.200610001.B